water

MDPI

Article

Sea Level Rise-Induced Transition from Rare Fluvial Extremes to Chronic and Compound Floods

Kazi Samsunnahar Mita [1,*], Philip Orton [1,*], Franco Montalto [2], Firas Saleh [3] and Julia Rockwell [4]

[1] Department of Civil, Environmental and Ocean Engineering, Stevens Institute of Technology, Hoboken, NJ 07030, USA
[2] Department of Civil, Architectural, and Environmental Engineering, Drexel University, Philadelphia, PA 19104, USA; fam26@drexel.edu
[3] Moody's RMS, 121 River St. #1300, Hoboken, NJ 07030, USA; firas.saleh1@gmail.com
[4] Climate Change Adaptation Program, Philadelphia Water Department, Philadelphia, PA 19107, USA; julia.rockwell@phila.gov
* Correspondence: kmita@stevens.edu (K.S.M.); porton@stevens.edu (P.O.); Tel.: +1-(347)-748-8553 (K.S.M.); +1-(212)-844-9009 (P.O.)

Abstract: Flooding is becoming more frequent along U.S. coastlines due to the rising impacts of fluvial and coastal flood sources, as well as their compound effects. However, we have a limited understanding of mechanisms whereby sea level rise (SLR) changes flood drivers and contributes to flood compounding. Additionally, flood mitigation studies for fluvial floodplains near tidal water bodies often overlook the potential future contribution of coastal water levels. This study investigates the role of SLR in inducing high-tide flooding (HTF) and compound flooding in a neighborhood that lies on a fluvial floodplain. Eastwick, Philadelphia, is a flood-prone neighborhood that lies on the confluence of two flashy, small tributaries of the tidal Delaware River. We develop a combined 1D-2D HEC-RAS fluvial-coastal flood model and demonstrate the model's accuracy for low-discharge tidal conditions and the extreme discharge conditions of tropical Cyclone (TC) Isaias (2020) (e.g., Root Mean Square Error 0.08 and 0.13 m, respectively). Simulations show that Eastwick may experience SLR-induced HTF as soon as the 2060s, and the flood extent (34.4%) could become as bad as present-day extreme event flooding (30.7% during TC Isaias) as soon as the 2080s (based on 95th percentile SLR projections). Simulations of Isaias flooding with SLR also indicate a trend toward compounding of extreme fluvial flooding. In both cases the coastal flood water enters Eastwick through a different pathway, over a land area not presently included in some fluvial flood models. Our results show that SLR will become an important contributor to future flooding even in fluvial floodplains near tidal water bodies and may require development of compound flood models that can capture new flood pathways.

Keywords: high-tide flooding; fluvial flooding; climate change; sea level rise; compound flooding

Citation: Mita, K.S.; Orton, P.; Montalto, F.; Saleh, F.; Rockwell, J. Sea Level Rise-Induced Transition from Rare Fluvial Extremes to Chronic and Compound Floods. *Water* **2023**, *15*, 2671. https://doi.org/10.3390/w15142671

Academic Editors: Chiara Favaretto, Claudia Cecioni and Maria Mimikou

Received: 15 June 2023
Revised: 9 July 2023
Accepted: 20 July 2023
Published: 24 July 2023

1. Introduction

Flooding is one of the costliest and deadliest natural hazards [1–3] affecting many regions around the world [4–6]. Coastal regions are particularly vulnerable to flooding impacts due to dense and rapidly growing population centers [7,8] and intensely developed urban land areas. Along with these factors, increases in sea level and rainfall intensity are also driving increased flooding. The Global Mean Sea Level (GMSL) has been rising and will continue to rise in this century under all the Shared Socioeconomic Pathways (SSPs) considered by Intergovernmental Panel on Climate Change (IPCC). Along much of the U.S. East Coast, the Relative Mean Sea Level (RMSL) rise is projected to be greater than GMSL [9]. The increase in RMSL increases the frequency of high-tide flooding [10,11] and the risk of compounding extreme flood events [6,8,12].

Traditionally, studies of flood impacts have mainly focused on extreme fluvial and coastal flood events separately [13–16]. For example, the standard flood hazard assessment framework of the U.S. Federal Emergency Management Agency (FEMA) is univariate [6,15,17,18]. FEMA fluvial flood hazard studies neglect the contribution of dynamic coastal water levels [6,19]. Even in univariate studies of large-scale fluvial floods, the local flood risk is underestimated by neglecting flow from smaller streams, using coarse resolution terrain data, and assuming simplistic physics of flood spreading [20]. According to Wing et al. [20], FEMA flood hazard area delineation studies thoroughly mapped the coastal flood hazard, but fluvial and pluvial flood hazard zones are incomplete nationwide.

Compounding of flooding from multiple sources (typically storm surge and streamflow) has gained significant recent attention [6,12,21,22]. There have been studies focusing on local [23–25], continental [26], and global scales [12] examining the correlation between rain and surge. Wahl et al. [26] found a significant increase in the number of compound flood events over the past century for some coastal locations. US studies suggest that the risk of compounding flood drivers is higher on the US East Coast [6,26]. In addition, future SLR projections [4,27,28] and rainfall intensity increases [27,29,30] imply the trend in increasing flood risk will likely continue [8].

SLR is also increasingly inducing flooding outside of extreme conditions. High-tide-flooding (HTF) (alternatively known as nuisance, sunny day, and recurrent tidal flooding) is of much lesser magnitude than major flooding [10,31]. However, small, frequent HTF events can cause significant property damage cumulatively [32]. Several studies suggested that HTF flood frequency has increased exponentially in the last 70 years [10,11,33], and it will continue to rise due to SLR [11,34,35] under various SSPs. According to Dahl et al. [33], in the next 15 to 30 years, many communities will face chronic HTF due to sea level rise which will later cause permanent inundation. Thompson et al. [24] reported the onset of rapid increase in HTF frequency from the mid-2030s onwards in the US. In some coastal regions, today's HTF and minor surge flooding have similar impacts compared to major surge or hurricane impacts in the past [28].

Local scale modeling and process studies of SLR impacts on compounding of extreme flood events and HTF have been understudied. Moreover, these studies have typically focused only on extreme flooding induced by tropical cyclones (TCs)/extreme coastal water level [4,21,36–39]. Numerical modeling of HTF, on the other hand, is still under-explored in flood research. A holistic focus on both extremes and chronic floods can better help reveal the full range of processes and effects of SLR on changing drivers and compounding floods. Monthly tidal flooding with SLR is a valuable metric representing the future onset of chronic flooding [40]. With the increase in frequency, depth, and extent of HTF in coastal urban neighborhoods, the importance of addressing HTF in flood management measures is also becoming imperative.

In this study, a model capable of simulating HTF, coastal, fluvial, and compound flooding is developed for a neighborhood historically impacted by fluvial flooding but increasingly at risk of coastal flooding. The model is validated using monthly high tide and an extreme rainfall event. The effects of SLR on tidal floods and the conversion of fluvial floods to compound floods are explored. This submission constitutes the first in a series focused on flood modeling, changing flood hazards, and potential flood risk mitigation solutions for the neighborhood of Eastwick, Philadelphia.

2. Study Area

Eastwick is a community of about 42,000 people in Southwest Philadelphia adjacent to Philadelphia International Airport (referred to as Airport in Figure 1b). Hydrologically, Eastwick is located at the confluence of the Darby and Cobbs Creeks which have watershed drainage areas of approximately 104 km^2 and 60 km^2, respectively. The hydrologic complexity in Eastwick arises from several features, including the elevated Clearview Landfill Superfund site located near the confluence ("landfill" in Figure 1b), the impounded John Heinz Wildlife Refuge (JHR in Figure 1b) further downstream, and the largest remaining

freshwater tidal marsh in Pennsylvania (in the LDC area in the Figure 1b). In addition to minor flooding events, heavy precipitation during tropical storms Floyd (1999), Irene (2011), Sandy (2012), and recent TC Isaias (2020) have caused extensive and severe flooding in this area. Based on U.S. Army Corps of Engineers (USACE) high water mark data and interactions between the research team and long-term residents, TC Floyd and TC Isaias were the first and second worst flooding events in Eastwick during the post-urban renewal period (~1960s to present). Eastwick's high susceptibility to flooding arises from its proximity to the Darby–Cobbs, the tidal Delaware River, and the Schuylkill River.

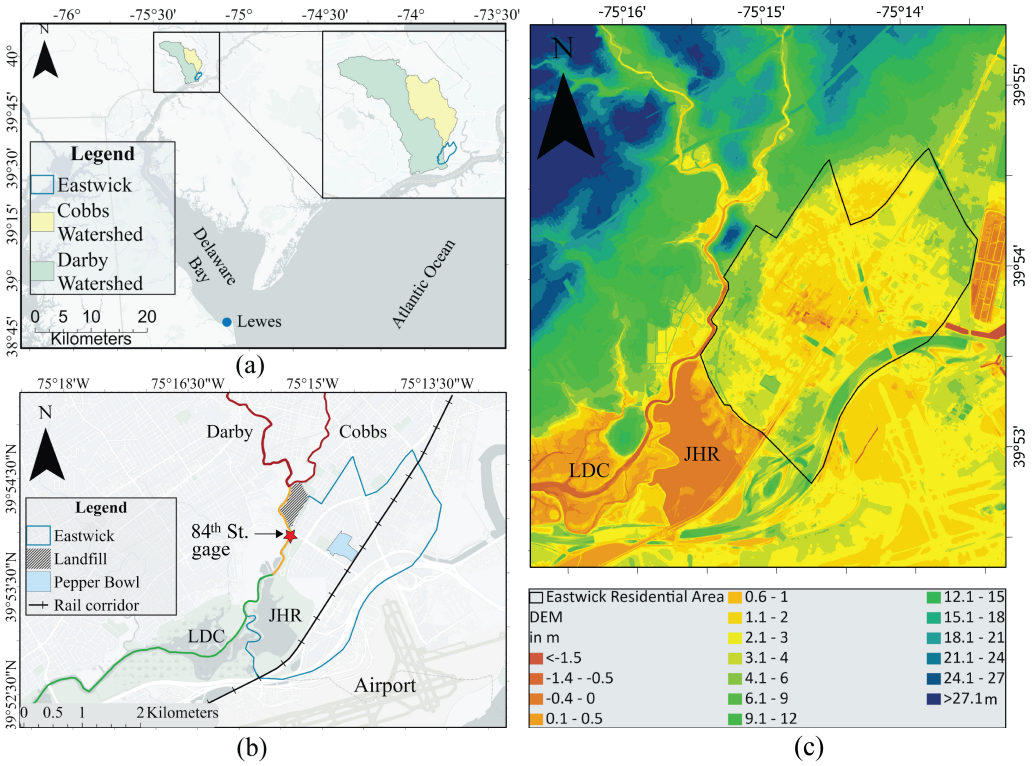

Figure 1. Map of the study area. (**a**) shows the location of Eastwick from the Atlantic Ocean including Delaware Bay and Rivers, and (**b**) shows Eastwick and some other local key features (JHR and LDC are acronym for John Heinz Wildlife Refuge and Lower Darby Creek respectively); red, yellow, and green lines show different Manning's roughness region along the creeks (discussed more in Section 3.1.5). (**c**) Digital Elevation Model (DEM) of the study area.

Flooding has been a longstanding and growing concern of the Eastwick community, and there have been multiple studies assessing flood risk and effectiveness of various adaptation measures [41–43]. USACE [41] conducted a hydraulic analysis of existing conditions and the impacts of a proposed levee (embankment). The USACE study represented the study area by cross-sections (1D model) and modeled steady flow during extreme hurricanes Floyd, Irene, and Lee. To improve the initial modeling effort and accurately represent multidimensional flows in the neighborhood, a Princeton Hydro [43] study represented the neighborhood (Figure 1b) as a 2D model domain keeping the channels 1D. Like this study, AKRF [42] modeled the neighborhood for redevelopment purposes as a 2D flow area but extended river reaches using a 1D model in both upstream and downstream directions. While modeling the river reach in 1D is computationally less expensive and adequate for regular flow conditions, the wetlands in the Darby–Cobbs system make the flow dynamics more complex, especially during extreme events [44,45]. So, to understand current and future flood pathways into Eastwick, in this study, we improve upon previous attempts and incorporate the Darby–Cobbs creeks as a 2D flow area extending the downstream boundaries to the Delaware river (Figure 2).

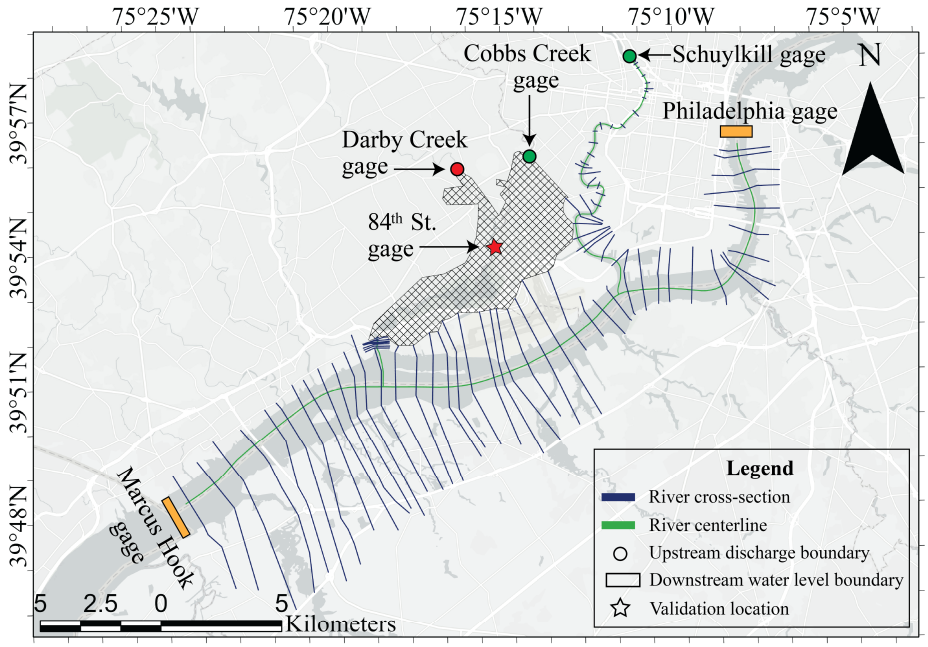

Figure 2. Model Domain. Cross-hatched polygon represents 2D model domain, and river cross-sections and centerline indicate 1D model domain. The circle represents discharge boundaries, and rectangles represent water level boundaries. Fill color red indicates limited data record (~5 years).

There have also been limited attempts to simulate coastal flooding in Eastwick. While the USACE [41] study did not address coastal events, Princeton Hydro [43] simulated a NOAA 1% storm and NOAA SLOSH category one storm with a 1D-2D HEC-RAS model. This analysis used a 1D model in the Lower Darby Creek and only allowed for Eastwick flooding from the 1D Darby river channel and not across the John Heinz Refuge (JHR) floodplain. Thus, the Princeton Hydro study does not capture the possible overflow location at the south end of Eastwick near the rail corridor (Figure 1b). AKRF [42] incorporated a few coastal events like TC Sandy, 1950 storm (in present and future SLR conditions), and two synthetic compound events. But their study, too, was limited by the unavailability of observed data during extreme events (described in Section 3.2.2). To deal with these limitations, the AKRF study made simplistic assumptions that involved scaling up/down the Isaias hydrograph to simulate these storms. While their model is the most detailed among all these published studies, the model is not validated. Our research is a continuation of previous efforts to study flood mitigation strategies in Eastwick. Through our research, we plan to address the shortcomings of prior studies and develop a model of Eastwick capable of simulating coastal, fluvial, and compound flooding efficiently. The project is a collaboration with Drexel University, Philadelphia Water Department (PWD), and the model has been shared [46] through workshops with PWD, Philadelphia Office of Sustainability, the US Army Corps of Engineers, local community organizations, and other partners.

3. Methodology

In this study, a widely used publicly available modeling tool HEC-RAS (v6.0) developed by the USACE is used. Many previous studies applied HEC-RAS to study compound flooding in different places around the world [5,29,37,47,48]. HEC-RAS has these unique capabilities of performing combined 1D-2D modeling within the same flow model which gives modelers the scope of using 1D in large river systems and 2D in areas requiring more accuracy in hydraulics, making the model computationally less expensive. The model was applied with full momentum balance mode in its 2D regions. The following sub-section describes the model set-up parameters; validation for regular and extreme flow conditions;

and analyses of the impacts of SLR on HTF and compounding of fluvial extreme flooding in Eastwick.

3.1. Model Set Up

3.1.1. Topo-Bathymetry Data of the Model

LIDAR-based topography data are merged with boat survey bathymetry data to form the model's digital elevation model (DEM) data in the Eastwick and Darby–Cobbs area. The topography comes from the Pennsylvania Spatial Data Archive [49] in the form of LIDAR (light detection and ranging) generated DEM of 1 m (3.28 ft) resolution. The bathymetry of the Delaware River, Schuylkill River, Darby Creek, and Cobbs Creek are collected from various sources. The channel bathymetries of Darby and Cobbs Creeks are incorporated from the 2014 USACE study. The channel bathymetry used in this study is developed by merging the PWD survey data from above the Darby–Cobbs confluence with Environmental Protection Agency (EPA) Bathymetry Survey data south of the confluence of Darby and Cobbs Creeks [41]. Bathymetries of the Delaware and Schuylkill River reaches are collected from National Oceanic and Atmospheric Administration (NOAA) National Centers for Environmental Information's (NCEI) combined topographic and bathymetric DEM data [50] and NOAA Nautical Charts [51]. Data are combined from these two sources using the Nautical Charts data as the base information and supplementing them with the NCEI data [42].

3.1.2. Upstream and Downstream Boundary Conditions

Model boundaries are placed in locations where existing discharge and/or water level gage stations exist. The upstream boundaries of the model are USGS gage stations [52]. For Darby Creek upstream boundary, USGS gage Darby Creek near Darby, PA (Gage ID: 01475510); for Cobbs Creek, Cobbs Creek at Mt. Moriah Cemetery, PA (Gage ID: 01475548); and for Schuylkill River, Schuylkill River at Philadelphia, PA (Gage ID: 01474500) have been used. The USGS gage at 84th Street (Gage ID: 01475553) is used as the model validation location. This station is the only operational gage station located within the model domain and adjacent to the area of interest. One constraining factor in modeling historic flooding in Eastwick is limited records. One of the contributing tributaries, the Darby Creek gage, has a time series of discharge data going back to only Nov 2018. The validation location, USGS 84th St. gage, has water level data records from 2017. These data constraints limit the number of events that can be simulated using observed data.

One of the challenges setting up the model was capturing the tide timing at Darby–Cobbs inlet (from the Delaware River) correctly. Initially the model was set up using only a 2D model domain (Figure 2). To set up the downstream boundary at the inlet, a simplistic assumption of progressive wave was used to offset tide gage data from Marcus Hook based on travel time to the NOAA tide gage station at Philadelphia. But the resulting tide phasing was delayed compared to observations at 84th St. To capture the tide phasing and propagation correctly, the 1D model of the Delaware and Schuylkill River is connected to the 2D model domain. The downstream boundaries in the Delaware River are tidal water level boundaries. The NOAA Philadelphia gage station and NOAA Marcus Hook gage stations are used as downstream boundary conditions in this study [53].

3.1.3. Grid Size

In the 2D model domain, 7.62 m × 7.62 m (25′ × 25′) model grid has been used. Levees require higher resolution and are defined by break lines aligned along their axis. For example, in the John Heinz National Wildlife Refuge (JHR in Figure 1b) where strong tidal flow occurs, grid cells near the break lines can have significantly smaller resolution 1.52 m × 1.52 m (5′ × 5′). Cells in HEC-RAS can have up to eight sides. Each cell is a detailed elevation volume/area relationship that represents the details of underlying terrain. Because of these high-resolution sub-grid features, wetted flood area will be based on underlying detailed terrain, not computational grid size. This feature of HEC-RAS

enables us to use comparatively coarser grid without compromising the accuracy of output. The 2D flow area comprises of nearly 467,562 cells.

3.1.4. Computational Time Step

Computational time step is another important parameter to attain a numerically stable model and good results. A too large time step causes numerical diffusion and may cause model instability. If the time step is too small, the computation time can be very long which is not desired in most cases. In this study, the time step of simulation 30 s has been chosen based on convergence test of numerical solutions for various time steps.

3.1.5. Land Cover and Land and Bed Roughness

In this study, land use data from National Land Cover Database (NLCD) collected in 2016 at a 30 m resolution are used [54]. Then, appropriate roughness values have been associated with various land use types (see Supplementary Materials Table S1a) [55]. For example, medium intensity developed region and Estuarine emergent wetland are assigned Manning's roughness of 0.1 and 0.05, respectively.

A physics-based approach was used to set reasonable Manning's roughness in river channels. In the 2D model domain, four regimes (shown in red, yellow, and green lines (Figure 1b)) are defined based coarsely on river slope, and Manning's numbers are roughly estimated for each based on prior studies, images of the creek bed, and the bed slope. The channel bed from upstream boundaries (both Darby and Cobbs) to confluence of Darby–Cobbs is relatively steeper (0.002) and has boulders and vegetation obstruction along the way. Bed material downstream of the confluence becomes finer gradually, and the bed slope declines to 0.001. To account for these differing substrates and their hydraulic effects, we applied Manning's roughness from range of possible values based on bed characteristics [56]. The Manning's n values used within the river channels are shown in Table S1b in Supplementary Materials.

3.2. Flood Events for Model Validation and Flood Mapping

3.2.1. Model Set Up for Tidal Flooding

The model is validated for a week-long spring tide period with low stream flows and a high coastal sea level anomaly of ~0.3 m at Lewes, Delaware, shown in Figure 1b (NOAA station 8557380). The peak water level of 1.56 m North American Vertical Datum of 1988 (NAVD88) is exceeded 14 times per year on average at 84th St. tide gauge (USGS station 8557380 data from 2017 to 2022), and we hereafter refer to this as monthly HTF [40]. The period of the simulation is from 24 August to 31 August 2019, and the average median daily discharge through Darby, Cobbs Creeks, and Schuylkill River during this period is 0.34 m^3/s, 0.79 m^3/s, and 33.7 m^3/s, respectively. The tidal boundary conditions at Philadelphia and Marcus hook gage are shown in Figure 3.

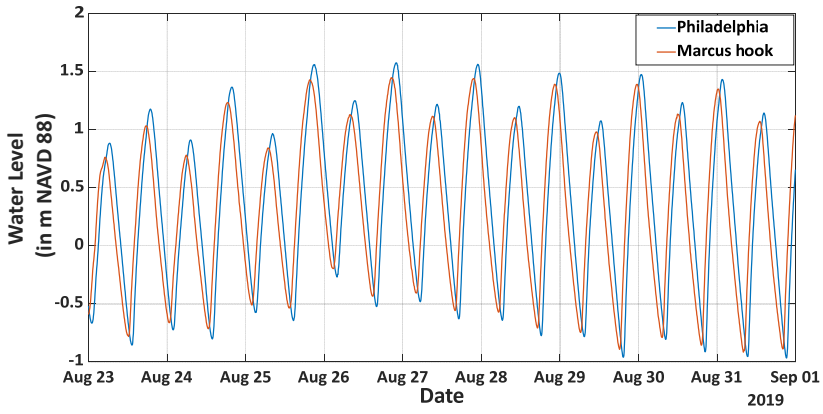

Figure 3. Tidal water level boundary conditions.

3.2.2. Model Set Up for TC Isaias

The model is validated for TC Isaias (2020) due to both the widespread severe flooding in Eastwick and the wider availability of useful data in comparison to earlier floods. TC Isaias was mainly a fluvial flood event with a return period of ~30 years, given that it was the second worst event in about 60 years of historical information (the Weibull unbiased empirical probability assumption; [57]). It was not an extreme event in terms of water level on the Delaware River, with a water level return period of about 2 years at the Philadelphia tide gauge. The Darby Creek upstream gage station has data from 2017, and the 84th St. gage used for model validation has data from late 2018 to present. Therefore, observed data for prior storms are significantly lacking. For Isaias, in addition to water level at 84th St., High Water Marks (HWMs) were collected by the USACE right after Isaias in Eastwick. The uncertainty of the HWMs is reported to be 0.06m (0.2 ft) which is classified as fair in quality assuring process [58].

The Isaias simulation includes scaled up streamflow following the recommendations of previous studies [41,43,59]. During extreme flow events, the accuracy of measured flow data at Mt. Moriah gage at Cobbs Creek and Darby Creek gage is questionable. In USACE [41,59] studies, it is mentioned that the flow measurement method at Mt. Moriah gage is reported to be indirect, indicating that reported discharge is an estimate based on either extrapolation or calculation. There is high suspicion that gage data at high flows may be impacted by the bridge downstream of the gage [41,59]. During high flow events, the water level at the bridge reaches the low steel above the opening, and the relationship used for calculation and extrapolation at the gage is affected. The USACE study [41] did not trust flow values in cases of extreme flow events and used a stage discharge relationship based on 1977 Flood Insurance Study (FIS) as an alternate method to convert measured peak stages to flows. At the time of the USACE study, the Darby Creek station was not operational. But there is similar suspicion about the current measured discharge data at this location too. Though this gage has observed flow data for Isaias, around the time of peak discharge, the gage discontinued logging observed data, and estimated discharge was provided instead. To test the claim, we simulated Isaias using USGS-provided discharge data which showed no flooding at all in Eastwick (see Supplementary Materials Figure S1). This is contrary to many media reports and USACE HWMs data. This analysis supports the claim that both gages are underestimating discharge during extreme flow events. Because of the uncertainties in observed data, we assumed that the recorded data could capture the shape and timing of the hydrographs at both gages but underestimate the flow magnitude in accordance with these prior studies [41,43]. So, the flows at Darby and Cobbs Creek are scaled up using the same methodology as USACE [41] in this study (Table 1).

Table 1. Summary of rating curve comparison at Mt Moriah gage location at Cobbs and Providence Road at Darby for TC Isaias.

Stream	Measured Stage (m)	WSE (in m NAVD 88)	Estimated Discharge from 1977 FIS Study (m^3/s)	Measured Discharge (m^3/s)	Coefficient
Cobbs	5.5	11.30	325.64	211.24	1.54
Darby	3.94	9.71	205.22	171.60	1.2

3.3. SLR Scenarios and Estimated Time of Arrival

To study the onset of tidal flooding in Eastwick, SLR scenarios ranging from 0.3 to 1.8 m with 0.3 m increment (integers between 1 to 6 ft) on top of a baseline in 2019 are considered in this study. Using a range of SLR values enables us to model the onset of tidal flooding in Eastwick and the progression of flooding as sea level rises.

Based on the latest IPCC Sixth Assessment Report (IPCC AR6) 2022 SLR projections for Philadelphia, decades when these SLR scenarios occur at 5th, 50th, and 95th percentiles are estimated. To create this decadal estimate, the available projection data are plotted against the year and regressions equation of 4th order polynomial for 5th percentile (R^2 = 0.998), lin-

ear for 50th percentile (R^2 = 0.999), and 2nd order polynomial for 95th percentile (R^2 = 0.999) are formulated. Using these regression equations, projected SLR for each year is calculated. Lastly, the SLR scenarios considered in this study and the corresponding projected decade of occurrence are obtained. The projection timeframe for each SLR scenario is useful for planning, implementation, and mitigation purposes.

3.4. Compounding of Extreme Fluvial Flooding Due to SLR

To study the compounding of extreme fluvial flood due to SLR, we simulated TC Isaias with 0.6 m (2 ft) and 1.2 m (4 ft) SLR. The spatial differences between maximum water level of base scenario and future scenarios are mapped and compared to understand the potential change in flood pathways due to SLR.

4. Results

4.1. Model Validation Results

4.1.1. Tide Validation

The HEC-RAS 1D-2D model has high accuracy for capturing the phase and high waters during the tide simulation (Figure 4). The modeled and observed water level has a root mean square error (RMSE) of 0.08 m, mean average error (MAE), and mean error (ME) of 0.04 m, respectively (Table 2). The Nash–Sutcliffe model efficiency coefficient (NSE) representing the predictive skill of model is calculated to be 0.97 (1.00 being a perfect model). But at times of low water (LW), the simulated water level does not reach the observed data, and there is a consistent bias of −0.1 m. However, we did not tune the model to get better results at LW because our focus is on high waters and floods. This bias in LW can be attributed to the uncertainty of the bathymetry data. There are localized uncertainties associated with the bathymetry of the river channel. The 84th St. gage is located on the bend of Darby Creek, and a point bar forms and erodes below the gage at the center pier periodically [41,43]. Because of the periodic formation and erosion of the point bar, there is a possibility of error in the surveyed bathymetry and overestimation/underestimation of LW levels.

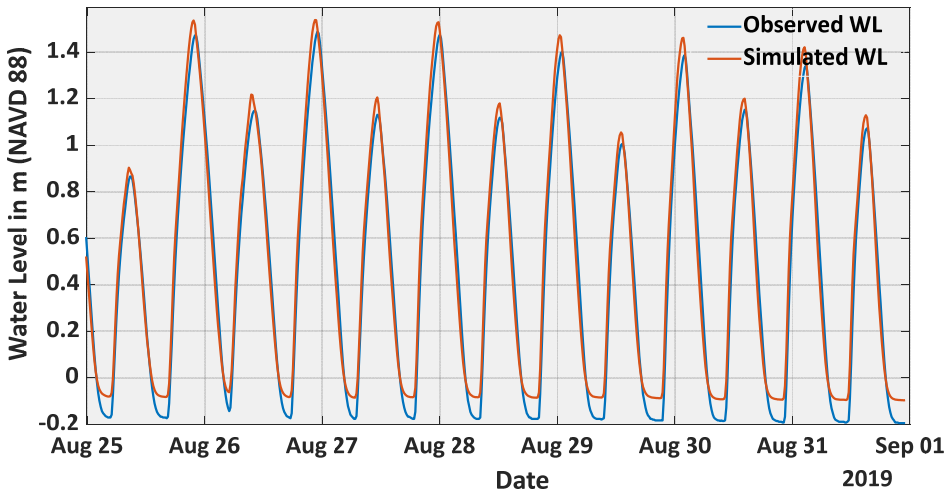

Figure 4. Water level comparison at USGS 84th St. gage.

Table 2. Summary of statistical indicators for different validation approaches.

Indicator \ Event	Monthly Tide	Extreme Flow Event Isaias	
	Tide Time Series	Isaias Time Series	High Water Marks
RMSE (m)	0.08	0.13	0.32
ME (m)	0.04	−0.08	0.28
MAE (m)	0.07	0.14	−0.09
NSE	0.97	0.98	-
R^2	-	-	0.8803

4.1.2. TC Isaias Validation

The model also has good accuracy for capturing the flooding extent in Eastwick based on the comparison with HWMs data (Figure 5). Figure 5a shows the model-simulated maximum inundation extent during TC Isaias. During flooding, the overtopping starts to occur near the confluence of Darby and Cobbs and inundates nearby streets and ultimately reaches the low-lying area in the middle of Eastwick, locally known as Pepper Bowl (Figure 1b,c). In Supplementary Materials Figure S2, the spatial distribution of high-water marks (HWMs) collected after TC Isaias is shown. The comparison between observed and modeled HWMs at every point is presented (Figure 5b). As it is seen from the results, the model simulated HWMs are consistent with surveyed HWMs with RMSE 0.32 m, ME of 0.28 m, MAE of HWM is 0.28 m, and R^2 of 0.88, which is a relatively good fit for a flood model and HWMs [15,60,61].

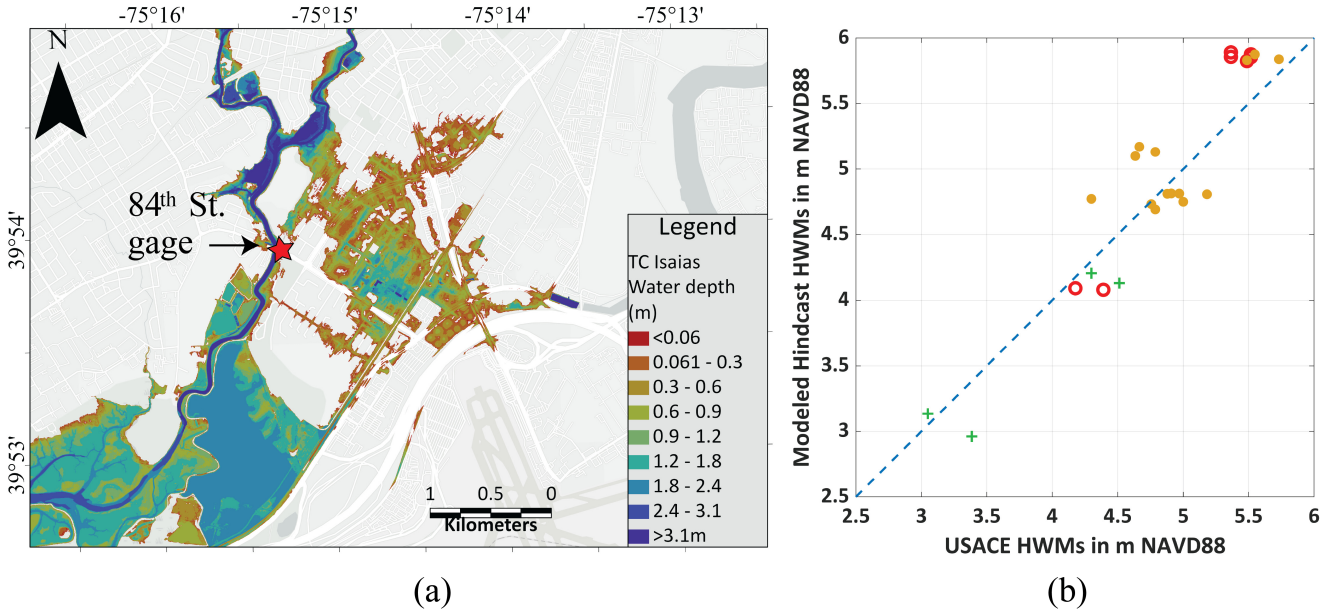

Figure 5. (**a**) Maximum inundation extent during Isaias. (**b**) Comparison of model-simulated HWMs with recorded HWMs. Color indicates closeness of points to the creek (red points are closest to the creek, and green denotes furthest ones; see Supplementary Materials Figure S2).

The water level time series during Isaias at 84th St. generally shows good agreement with observed data, except for a discrepancy at the peak (Figure 6). To quantify the model's performance during extreme flow event, we used a segment of time series around the peak to calculate the statistical indicators (black dashed portion in Figure 6). The RMSE, MAE, ME, and NSE of the model in this extreme flow scenario are 0.13 m, −0.08 m, 0.14 m, and 0.98, respectively (Table 2). Similar to the time series of the tidal water level, the water level during Isaias also has some discrepancy during low tide, which can be attributed to the bathymetry uncertainty as discussed in Section 4.1.1. Another source of uncertainty

comes from the estimation of upstream discharge based on the methodology described in Section 3.2.2. The 0.14 m difference in peak water level with observation can be caused by this reason or complexities of the bridge itself that may be obstructing flow. Simulating extreme flows below bridges with potential debris trapping and morphologic changes can be a challenging topic [62,63].

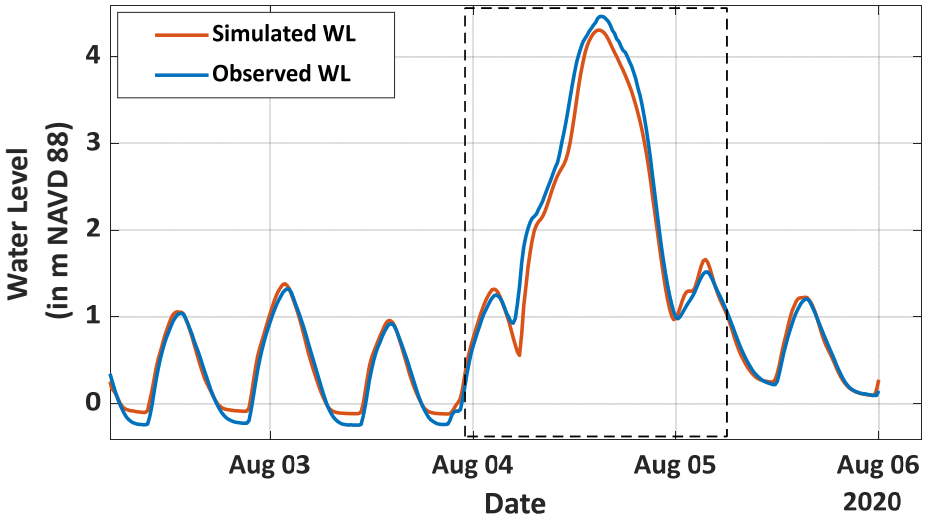

Figure 6. Water level comparison at USGS 84th St. gage during Isaias. Black dashed portion represents data used to calculate the statistical indicators in Table 2.

4.2. Future Impact of SLR on Tidal Flooding

The tide simulation (described in Section 3.2.1) with added SLR demonstrates that monthly HTF will eventually begin to affect Eastwick after an additional 0.6 m of SLR and increasingly with further SLR increments (Figure 7). Analyses of the modeled flood pathway show that water starts to propagate from JHR through the rail corridor (indicated in Figure 1b) and ponds in the 'Pepper Bowl' of Eastwick (indicated in Figure 1b). As the magnitude of SLR grows, the depth of water in and around Pepper Bowl increases, as does the total flooding extent. Table 3 below shows the tidally flooded area for a range of SLR scenarios. For 0.6 m of SLR, about 3% of Eastwick is flooded, whereas for 0.9 m of SLR, the total flooded area increases to more than 18%. With 1.2 m of SLR, the flood extent (34.4% of Eastwick) becomes greater than that for Isaias (30.7% of Eastwick). Additional SLR (1.5 and 1.8 m) causes about half of Eastwick to experience chronic HTF.

Table 3. Various tidal and flow scenarios resulting in inundated area (in %) in Eastwick. Raster cells greater than 3 cm are considered wet for inundated area calculation.

Flow Conditions	Scenario	Inundated Area (%)
SLR scenarios	0.3 m (1 ft)	~0
	0.6 m (2 ft)	3.1
	0.9 m (3 ft)	18.6
	1.2 m (4 ft)	34.4
	1.5 m (5 ft)	46.1
	1.8 m (6 ft)	57.9
Isaias (2020)	Isaias	30.7

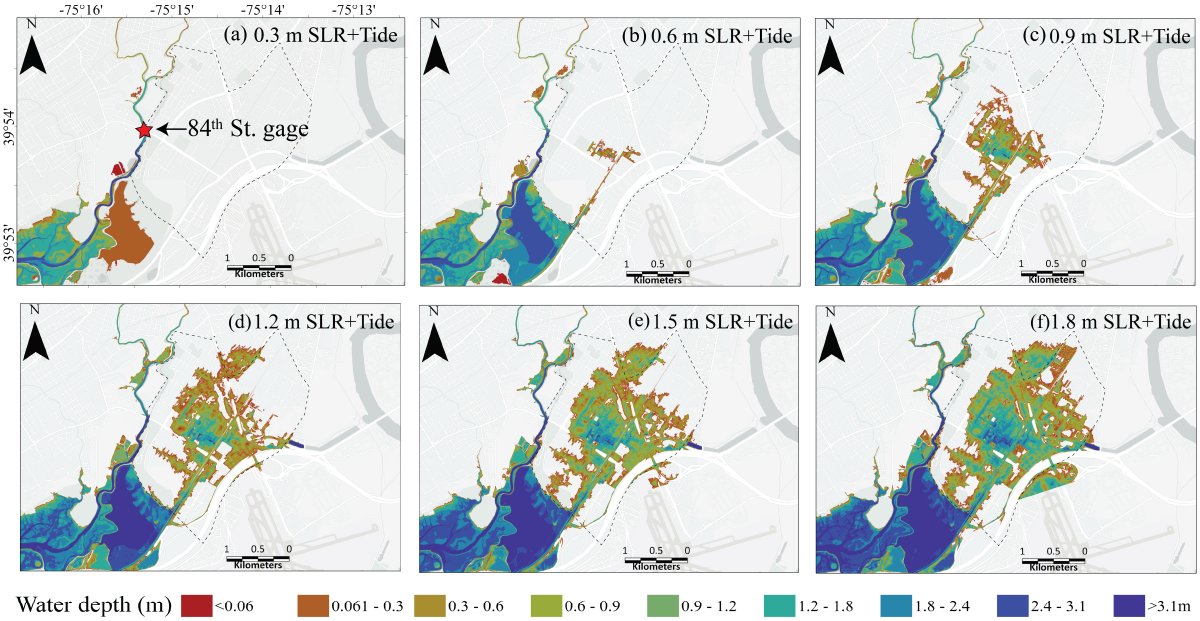

Figure 7. Monthly high-tide flooding with various sea level rise (SLR) scenarios (see caption on top left). Depths shown are temporal maxima of the monthly high-tide simulations. All sub-figures have the same spatial extent.

Estimated Decade for Each SLR Scenario

According to Tables 3 and 4, some areas of Eastwick might start experiencing monthly HTF due to SLR as soon as the 2060s. As the flooding extent expands with increasing SLR, Isaias-like flooding may occur monthly by the 2080s under a high-end SLR scenario. If other anthropogenic factors such as dredging or shoreline hardening cause the tidal high-water levels to rise, similar flooding can occur sooner [64–66].

Table 4. SLR scenarios and approximate decadal timing for the 5th, 50th, and 95th percentile projections. MSL 2019 is 0.28 m NAVD88.

SLR in m (above MSL 2019)	Low End (5 Percentiles)	Median (50 Percentiles)	High End (95 Percentiles)
0.3	2080s	2050s	2040s
0.6	>2150	2090s	2060s
0.9	>2150	2130s	2070s
1.2	>2150	>2150	2080s
1.5	>2150	>2150	2100s
1.8	>2150	>2150	2110s

Note(s): SLR estimate over NAVD 88 datum.

4.3. Compounding of Extreme Fluvial Flooding under SLR Scenarios

For this analysis, we compared flooding during Isaias in base (2020) and future SLR (0.6 m, 1.2 m) scenarios. Figure 8a shows the coastal water contribution to flood water depth during Isaias in the 2D model domain. Overall, the approximately 2-year return period storm tide did not compound the fluvial flooding in Eastwick significantly. Along the creeks, from JHR to upstream of creeks and in the flooded area, the flood water depth remains unchanged due to the presence of storm tide. Storm tide compounds the water depth in LDC, surrounding wetlands, and JHR (Figure 1b) by various degrees: from a few centimeters in Eastwick to up to 1 m near the downstream boundary.

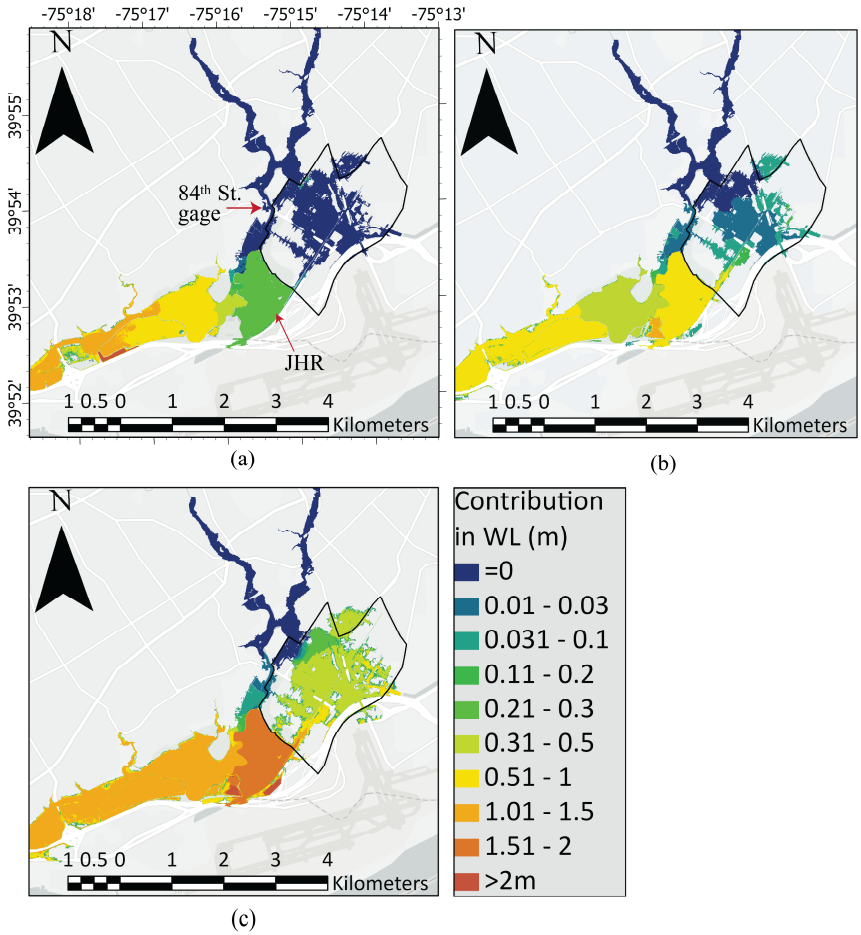

Figure 8. Contribution in rise in water level during Isaias (**a**) due to the coastal contribution in the base scenario, (**b**) due to coastal contribution of 0.6 m SLR, and (**c**) 1.2 m SLR scenario, respectively. All sub-figures have the same spatial extent.

For Isaias occurring with 0.6 m of SLR (Figure 8b), the water depth increases in various degrees along the channel up to 84th St. (water depth ranging from about 0.5 m to few centimeters). In Eastwick, the increased water travels along the rail corridor, and water depth gets increased by <10 cm in most places to up to about 1 m near the rail corridor. From 84th St. to upstream, boundaries and overflow region near the landfill are unaffected by 0.6 m SLR. In this SLR scenario, JHR acts as a water retention basin as the comparison between Figure 8a,b shows a significant increase in water depth. For Isaias with 1.2 m of SLR, the effect of compounding reaches slightly northward near the landfill (comparison along the channel between Figure 8b,c). The water depth increases within the range of 10 s of cm to about 1.5 m inside Eastwick. In the downstream region, water depth increases about 1.5 m or less. A little newly flooded area near the airport accumulates water up to 2 m. This analysis shows that during an extreme event like Isaias, SLR will mainly cause additional flooding from downstream (through JHR along the rail corridor). In the present-day condition, Eastwick gets flooded from Cobbs Creek near the confluence of Darby and Cobbs (Figure 8a). Our analysis shows that SLR does not directly contribute to water level along the current overflow path into Eastwick. However, it will potentially create a new overflow path from downstream and exacerbate the flooding conditions. This illustrates that even a two-year return period storm tide event can exacerbate an extreme fluvial flood in future SLR conditions.

5. Discussion

This study develops a flood model of coastal and fluvial flooding for flood-prone Eastwick and applies it to study how SLR will affect tidal and fluvial flooding. A high-resolution 1D-2D fluvial-coastal flood model is developed to efficiently capture the hydraulics of the study area. We show accurate validations for two separate events: (i) monthly tidal event and (ii) extreme fluvial flood event Isaias. Results show high fidelity in replicating flooding conditions with time series RMSE of 0.08 m for tides (Figure 4) and 0.13 m for Isaias (Figure 6), the latter of which is similar to prior flood modeling studies [5,21,60]. This is a collaborative research project with Drexel University and the Philadelphia Water Department (PWD), and the model has been shared [46] through workshops with PWD, Philadelphia Office of Sustainability, the US Army Corps of Engineers, and others, who are either using our model to directly inform Eastwick planning efforts or have replicated aspects of our model in their own projects.

The results demonstrate a case where SLR can lead to chronic HTF and compounding of fluvial extreme floods in a fluvial floodplain. Prior research has demonstrated how SLR causes increased high-tide flood frequency and area [10,28,33], but little research has investigated the transition from fluvial extremes to high-tide flooding. Below, we discuss this further in Section 5.1. An important finding here is that the pathway by which coastal compounding of fluvial floods occur is outside the river channel, across a complicated floodplain. This water pathway may not be captured by models originally developed to study the purely riverine-driven flooding, such as that used by the USACE [41] in an ongoing flood risk reduction study. This is further discussed in Section 5.2.

Our modeling of the Isaias fluvial flood neglects both pluvial flood water and the stormwater drainage system, which during extreme rain events like Isaias likely leads to relatively small errors that partially counteract each other. A previous study of Isaias by AKRF [67] evaluated the flood water volume budget and showed that the total storm sewer volume is very low compared to extreme runoff volume. Additionally, the combined area of the Darby–Cobbs watershed is about 10 times larger than the area of Eastwick (Figure 1a), so the local pluvial source is also likely a relatively small fraction of all floodwaters. Modeling rain on the model grid requires significant additional computational power on our 2D model domain, and we have chosen to neglect it due to our broader project's goal of simulating hundreds of flood events for risk and adaptation assessment. From our perspective, allowing rain on grid modeling without incorporating the stormwater pipe networks will also show overestimation of flooding. Moreover, our HWM validation is very accurate, so our simulation represents a very good representation of Isaias flooding. In addition, the neglect of rain and stormwater system should have a minimal impact on the specific conclusions of this research.

5.1. Impact of SLR in a Fluvial Flood Prone Coastal Area

This paper demonstrates that SLR can lead to chronic HTF in a fluvial floodplain and compounding of fluvial extreme floods. Previous studies of Eastwick focused on fluvial extreme events and ignored [41] or greatly oversimplified the effect of SLR by only looking at the coastal 100-year flood event [43]. In this analysis, we illustrate the inception and gradual progression of tidal flooding over a range of SLR scenarios in Eastwick (Figure 7). With only 0.6 m of SLR, Eastwick will start experiencing monthly HTF flooding, and this could occur as soon as the 2060s. Eastwick is an example of communities that will be affected by SLR-induced HTF as predicted in Dahl et al. [33] and Thompson et al. [24], although there is no historical case of Eastwick experiencing a coastal flood.

Moreover, consistent with what was demonstrated by Sweet and Park [28], our results illustrate that future, regularly occurring tidal floods in Eastwick can be as extensive as today's extreme fluvial floods. According to SLR projections, as soon as the 2080s, current day Isaias-like flooding can become a frequent phenomenon in Eastwick. Because of the high frequency of occurrence, HTF can cause more cumulative damage than infrequent extreme flood events [17].

In the case of extreme fluvial flood, SLR causes a shift towards flood compounding from the coastal source. In the analysis of impact of SLR in extreme fluvial flood like Isaias, first we study the influence of present-day tide in the water level inside the model domain. The result (Figure 8a) shows that the overtopping region and flooded area in Eastwick is predominantly driven by river flow. But with imposed SLR of 0.6 m and 1.2 m (Figure 8b,c), it is seen that the flood water depth in Eastwick increases significantly compared to the increase in the water level along the creek channel. SLR-driven higher tide exacerbates the flooding from Eastwick, directing additional flooding from the downstream breach location (along railroads in Figure 1b). This indicates that Eastwick will be prone to more flooding during extreme events in the future, and the additional flooding due to SLR will have more compounding characteristics.

5.2. New Pathways: An Additional Compound Flood Modeling Challenge

An additional challenge for modeling future compound flooding is that rising sea levels can lead to new floodwater pathways outside of river channels. Not only is compounding often neglected in flood-risk assessment and mitigation studies, but past models may not be capable of capturing these novel flood pathways. Only one recent study of Eastwick for redevelopment purposes by AKRF [42,67] initially incorporated compounding effects of sea level rise into a fluvial flood model with some simplistic assumptions. Because of less computational expense, 1D and 1D-2D flood modeling is very popular in fluvial flood related studies [5,29,37,48]. However, 1D or 1D-2D models based on existing flood flow pathways may overlook new flood pathways emerging from alterations in flood drivers. For example, because of not placing the lateral connection between 1D-2D flow area, the Princeton Hydro [43] study would not capture the flow pathway along the rail corridor. AKRF [42], on the other hand, captured this pathway because of connecting the 2D area with 1D cross sections.

The design of flood mitigation measures without considering possible HTF and compounding of extreme floods might not provide adequate protection in the future. For example, the current proposed USACE ([41,59]; and current ongoing work) mitigation measure for Eastwick is building a levee along the overtopping region north of the landfill in Eastwick. A levee can be effective in reducing the impact of fluvial flood, but with time, as the impact of SLR becomes more observable, residents of Eastwick will be facing frequent HTF and flooding from coastal sources along novel pathways.

6. Summary and Conclusions

This study investigates the impact of SLR in high-tide flooding and compounding of extreme flooding in a historically fluvially flooded area. An efficient 1D-2D HEC-RAS model is developed based on the best available data and made publicly available. The 1D-2D approach effectively captures the flooding in Eastwick with correct tide phase in the creeks. The model is validated for two events: (i) regular high-tide event and (ii) extreme flow event TC Isaias. To overcome the scarcity of good quality observed data, a scaled-up flow estimation approach used by USACE is used to estimate the flow during extreme event TC Isaias. Model results accurately replicate the water level time series and high water marks with RMSE 0.08 m for tide, 0.13 m for Isaias time series, and 0.32 m for Isaias high water marks inside Eastwick. The ME values are 0.04, −0.08, and 0.28 m, and the MAE values are 0.07, 0.014, and −0.09 m for these respective validation datasets. The error in the low waters can be attributed to the uncertainty in the river bathymetry below the 84th St. gage location.

This paper demonstrates that SLR can lead to chronic monthly HTF and compounding of fluvial extreme floods in what is presently only a fluvial floodplain. In the investigation of the impact of sea level rise in high-tide flooding, we found that Eastwick can start experiencing high-tide flooding as soon as the 2060s based on IPCC 2022 SLR projections. The total flooded area will increase rapidly and, in the 2080s, Eastwick may be experiencing high-tide flooding that is similar in extent (34.4%) to today's extreme fluvial flooding

(30.7%). Fluvial extreme flooding also gets compounded due to SLR. For an Isaias -like extreme event with 0.6 m of SLR, the water level gets increased by <10 cm in most places inside Eastwick except for along a rail corridor where the water level increases up to 1 m compared to the base scenario. With 1.2 m of SLR, the water level increases by 30–50 cm in most places, reaching 1.5 m in the most vulnerable places. In both cases of SLR-driven monthly HTF and extreme flooding, JHR retains flood water, and any excess water enters Eastwick from a new pathway. The 2D representation of the Lower Darby Creek and its neighboring wetlands enables us to identify this new flow pathway. The impact of SLR and alteration in flood pathways has rarely been considered in flood-related studies in Eastwick. All the current adaptation plans address protection from upstream riverine overflow only. However, our analysis suggests that SLR will be an important flood driver in the future, causing HTF and compound flooding, and, hence, needs to be incorporated in future flood protection plans.

A better understanding of the future changes in flood sources and pathways is crucial to identifying effective, long-term, and holistic flood risk mitigation measures. Fragmented approaches towards flood risk reduction need to be replaced by a more integrated approach [68,69]. Several studies have argued for the need for investing in holistic adaptation now to avoid greater costs in the future [70,71]. The application of bi/multivariate flood hazard assessments considering climate change effects can lead to improved design and testing for flood mitigation measures. Places at risk of facing more compounding of flooding in the next few decades, similar to Eastwick, should be studied, and the implementation of effective adaptation measures should be prioritized.

Supplementary Materials: The following supporting information can be downloaded at: https://www.mdpi.com/article/10.3390/w15142671/s1, Table S1: Manning's roughness with (a) various land use types (b) channel sections; Figure S1: Temporal maxima flooding of USGS measured flow-forced model of Isaias; Figure S2: Location of High-Water Marks of Isaias in Eastwick neighborhood collected by USACE.

Author Contributions: Conceptualization, P.O. and K.S.M.; methodology, P.O. and K.S.M.; software, K.S.M. and F.S.; validation, K.S.M.; formal analysis, K.S.M.; investigation, K.S.M. and P.O.; resources, P.O., F.M. and J.R.; writing—original draft preparation, K.S.M.; writing—review and editing, K.S.M., P.O., F.M., F.S. and J.R.; visualization, K.S.M.; supervision, P.O.; project administration, P.O., F.M. and J.R.; funding acquisition, P.O., F.M. and J.R. All authors have read and agreed to the published version of the manuscript.

Funding: This research was funded by the NOAA Climate Program Office Coastal and Ocean Climate Applications (NA19OAR4310307) and Climate Adaptation Partnerships (formerly the RISA program; NA21OAR4310313) grants.

Data Availability Statement: All data used in this study are available through public repositories. The DEM data is downloaded from https://www.pasda.psu.edu (accessed on 12 June 2023). For mentioned USGS gages, data are downloaded from https://waterdata.usgs.gov/nwis (accessed on 12 June 2023). Water level data are collected from NOAA https://tidesandcurrents.noaa.gov (accessed on 12 June 2023). The land use dataset is obtained from https://www.mrlc.gov (accessed on 12 June 2023). The current version of the model is shared in public domain: https://data.mendeley.com/datasets/3wjvmymf68/2 (accessed on 12 June 2023).

Acknowledgments: The authors would like to thank Philadelphia Water Department, U.S. Army Corps of Engineers, AKRF, Princeton Hydro, and United States Geophysical Survey for sharing information throughout the project. Authors greatly appreciate the active participation of Eastwick community members at various stages of the research for sharing their insights and thoughts. The statements made in this publication reflect solely the views of the individual authors and not the views of Risk Management Solutions, Inc., or its affiliates.

Conflicts of Interest: The authors declare no conflict of interest.

References

1. Bryant, E. *Natural Hazards*, 2nd ed.; Cambridge University Press: Cambridge, UK, 2005.
2. Whitfield, P. Floods in future climates: A review. *J. Flood Risk Manag.* **2012**, *5*, 336–365. [CrossRef]
3. Gaume, E.; Borga, M.; Carmen Llassat, M.; Maouche, S.; Lang, M.; Diakakis, M. *Mediterranean Extreme Floods and Flash Floods. A Scientific Update Coll. Synthèses*; Thiébault, S., Moatti, J.-P., Eds.; Institut de Recherche Pour le Développement: Marseille, France, 2016; pp. 133–144. Available online: https://hal.archives-ouvertes.fr/hal-01465740 (accessed on 12 June 2023).
4. Bilskie, M.V.; Hagen, S.C. Defining Flood Zone Transitions in Low-Gradient Coastal Regions. *Geophys. Res. Lett.* **2018**, *45*, 2761–2770. [CrossRef]
5. Pasquier, U.; He, Y.; Hooton, S.; Goulden, M.; Hiscock, K.M. An integrated 1D–2D hydraulic modelling approach to assess the sensitivity of a coastal region to compound flooding hazard under climate change. *Nat. Hazards* **2019**, *98*, 915–937. [CrossRef]
6. Moftakhari, H.R.; Salvadori, G.; AghaKouchak, A.; Sanders, B.F.; Matthew, R.A. Compounding effects of sea level rise and fluvial flooding. *Proc. Natl. Acad. Sci. USA* **2017**, *114*, 9785–9790. [CrossRef]
7. Martinich, J.; Neumann, J.; Ludwig, L.; Jantarasami, L. Risks of sea level rise to disadvantaged communities in the United States. *Mitig. Adapt. Strat. Glob. Chang.* **2013**, *18*, 169–185. [CrossRef]
8. Santiago-Collazo, F.L.; Bilskie, M.V.; Hagen, S.C. A comprehensive review of compound inundation models in low-gradient coastal watersheds. *Environ. Model. Softw.* **2019**, *119*, 166–181. [CrossRef]
9. Sweet, W.V.; Kopp, R.E.; Weaver, C.P.; Obeysekera, J.; Horton, R.M.; Thieler, E.R.; Zervas, C.; Kopp, R.E.; Weaver, C.P.; Obeysekera, J.; et al. *Global and Regional Sea Level Rise Scenarios for the United States*; NOAA Tech. Rep. NOS CO-OPS 083; National Oceanographic and Atmospheric Administration: Silver Spring, MD, USA, 2017.
10. Li, S.; Wahl, T.; Talke, S.A.; Jay, D.A.; Orton, P.M.; Liang, X.; Wang, G.; Liu, L. Evolving tides aggravate nuisance flooding along the U.S. coastline. *Sci. Adv.* **2021**, *7*, eabe2412. [CrossRef] [PubMed]
11. Moftakhari, H.R.; AghaKouchak, A.; Sanders, B.F.; Feldman, D.L.; Sweet, W.; Matthew, R.A.; Luke, A. Increased nuisance flooding along the coasts of the United States due to sea level rise: Past and future. *Geophys. Res. Lett.* **2015**, *42*, 9846–9852. [CrossRef]
12. Ward, P.J.; Couasnon, A.; Eilander, D.; Haigh, I.D.; Hendry, A.; Muis, S.; Veldkamp, T.I.E.; Winsemius, H.C.; Wahl, T. Dependence between high sea-level and high river discharge increases flood hazard in global deltas and estuaries. *Environ. Res. Lett.* **2018**, *13*, 084012. [CrossRef]
13. Alfieri, L.; Burek, P.; Dutra, E.; Krzeminski, B.; Muraro, D.; Thielen, J.; Pappenberger, F. GloFAS—Global ensemble streamflow forecasting and flood early warning. *Hydrol. Earth Syst. Sci.* **2013**, *17*, 1161–1175. [CrossRef]
14. Sampson, C.C.; Smith, A.M.; Bates, P.D.; Neal, J.C.; Alfieri, L.; Freer, J.E. A high-resolution global flood hazard model. *Water Resour. Res.* **2015**, *51*, 7358–7381. [CrossRef] [PubMed]
15. Wing, O.E.; Sampson, C.C.; Bates, P.D.; Quinn, N.; Smith, A.M.; Neal, J.C. A flood inundation forecast of Hurricane Harvey using a continental-scale 2D hydrodynamic model. *J. Hydrol. X* **2019**, *4*, 100039. [CrossRef]
16. Winsemius, H.C.; Aerts, J.C.J.H.; Van Beek, L.P.H.; Bierkens, M.F.P.; Bouwman, A.; Jongman, B.; Kwadijk, J.C.J.; Ligtvoet, W.; Lucas, P.L.; Van Vuuren, D.P.; et al. Global Drivers of Future River Flood Risk. *Nat. Clim. Chang.* **2016**, *6*, 381–385. [CrossRef]
17. Moftakhari, H.R.; AghaKouchak, A.; Sanders, B.F.; Allaire, M.; Matthew, R.A. What Is Nuisance Flooding? Defining and Monitoring an Emerging Challenge. *Water Resour. Res.* **2018**, *54*, 4218–4227. [CrossRef]
18. Gilles, D.; Young, N.; Schroeder, H.; Piotrowski, J.; Chang, Y.-J. Inundation Mapping Initiatives of the Iowa Flood Center: Statewide Coverage and Detailed Urban Flooding Analysis. *Water* **2012**, *4*, 85–106. [CrossRef]
19. *FEMA Guidance for Flood Risk Analysis and Mapping Combined Coastal and Riverine Floodplain*; Guidance report no. 60; Federal Emergency Management Agency: Washington, DC, USA, 2020.
20. Wing, O.E.J.; Bates, P.D.; Smith, A.M.; Sampson, C.C.; Johnson, K.A.; Fargione, J.; Morefield, P. Estimates of present and future flood risk in the conterminous United States. *Environ. Res. Lett.* **2018**, *13*, 034023. [CrossRef]
21. Orton, P.; Georgas, N.; Blumberg, A.; Pullen, J. Detailed modeling of recent severe storm tides in estuaries of the New York City region. *J. Geophys. Res. Oceans* **2012**, *117*, 1–17. [CrossRef]
22. Zscheischler, J.; Westra, S.; Van Den Hurk, B.J.J.M.; Seneviratne, S.I.; Ward, P.J.; Pitman, A.; AghaKouchak, A.; Bresch, D.N.; Leonard, M.; Wahl, T.; et al. Future climate risk from compound events. *Nat. Clim. Chang.* **2018**, *8*, 469–477. [CrossRef]
23. Klerk, W.J.; Winsemius, H.C.; Van Verseveld, W.J.; Bakker, A.M.R.; Diermanse, F. The co-incidence of storm surges and extreme discharges within the Rhine–Meuse Delta. *Environ. Res. Lett.* **2015**, *10*, 035005. [CrossRef]
24. Thompson, C.M.; Frazier, T.G. Deterministic and probabilistic flood modeling for contemporary and future coastal and inland precipitation inundation. *Appl. Geogr.* **2014**, *50*, 1–14. [CrossRef]
25. Zheng, F.; Westra, S.; Leonard, M.; Sisson, S.A. Modeling dependence between extreme rainfall and storm surge to estimate coastal flooding risk. *Water Resour. Res.* **2014**, *50*, 2050–2071. [CrossRef]
26. Wahl, T.; Jain, S.; Bender, J.; Meyers, S.D.; Luther, M.E. Increasing risk of compound flooding from storm surge and rainfall for major US cities. *Nat. Clim. Chang.* **2015**, *5*, 1093–1097. [CrossRef]
27. Karamouz, M.; Zahmatkesh, Z.; Goharian, E.; Nazif, S. Combined Impact of Inland and Coastal Floods: Mapping Knowledge Base for Development of Planning Strategies. *J. Water Resour. Plan. Manag.* **2015**, *141*, 04014098. [CrossRef]
28. Sweet, W.V.; Park, J. From the extreme to the mean: Acceleration and tipping points of coastal inundation from sea level rise. *Earth's Futur.* **2014**, *2*, 579–600. [CrossRef]

29. Feng, Y.; Brubaker, K.L. Sensitivity of Flood-Depth Frequency to Watershed-Runoff Change and Sea-Level Rise Using a One-Dimensional Hydraulic Model. *J. Hydrol. Eng.* **2016**, *21*, 05016015-1–05016015-8. [CrossRef]
30. Reidmiller, D.R.; Avery, C.W.; Easterling, D.R.; Kunkel, K.E.; Lewis, K.L.M.; Maycock, T.K.; Stewart, B.C. *Impacts, Risks, and Adaptation in the United States: The Fourth National Climate Assessment*; U.S. Global Change Research Program: Washington, DC, USA, 2018; Volume II, pp. 88–92. [CrossRef]
31. Sweet, W.; Dusek, G.; Obeysekera, J.T.B.; Marra, J.J. *Patterns and Projections of High Tide Flooding along the U.S. Coastline Using a Common Impact Threshold*; NOAA technical report NOS CO-OPS 086; National Oceanic and Atmospheric Administration: Washington, DC, USA, 2018. [CrossRef]
32. Moftakhari, H.R.; AghaKouchak, A.; Sanders, B.F.; Matthew, R.A. Cumulative hazard: The case of nuisance flooding. *Earth's Futur.* **2017**, *5*, 214–223. [CrossRef]
33. Dahl, K.A.; Fitzpatrick, M.F.; Spanger-Siegfried, E. Sea level rise drives increased tidal flooding frequency at tide gauges along the U.S. East and Gulf Coasts: Projections for 2030 and 2045. *PLoS ONE* **2017**, *12*, e0170949. [CrossRef]
34. Vandenberg-Rodes, A.; Moftakhari, H.R.; AghaKouchak, A.; Shahbaba, B.; Sanders, B.F.; Matthew, R.A. Projecting nuisance flooding in a warming climate using generalized linear models and Gaussian processes. *J. Geophys. Res. Oceans* **2016**, *121*, 8008–8020. [CrossRef]
35. Thompson, P.R.; Widlansky, M.J.; Hamlington, B.D.; Merrifield, M.A.; Marra, J.J.; Mitchum, G.T.; Sweet, W. Rapid increases and extreme months in projections of United States high-tide flooding. *Nat. Clim. Chang.* **2021**, *11*, 584–590. [CrossRef]
36. Kerr, P.C.; Westerink, J.J.; Dietrich, J.C.; Martyr, R.C.; Tanaka, S.; Resio, D.T.; Smith, J.M.; Westerink, H.J.; Westerink, L.G.; Wamsley, T.; et al. Surge Generation Mechanisms in the Lower Mississippi River and Discharge Dependency. *J. Waterw. Port Coast. Ocean Eng.* **2013**, *139*, 326–335. [CrossRef]
37. Gori, A.; Lin, N.; Xi, D. Tropical Cyclone Compound Flood Hazard Assessment: From Investigating Drivers to Quantifying Extreme Water Levels. *Earth's Futur.* **2020**, *8*, e2020EF001660. [CrossRef]
38. Bush, S.T.; Dresback, K.M.; Szpilka, C.M.; Kolar, R.L. Use of 1D Unsteady HEC-RAS in a Coupled System for Compound Flood Modeling: North Carolina Case Study. *J. Mar. Sci. Eng.* **2022**, *10*, 306. [CrossRef]
39. Brempong, E.K.; Almar, R.; Angnuureng, D.B.; Mattah, P.A.D.; Jayson-Quashigah, P.-N.; Antwi-Agyakwa, K.T.; Charuka, B. Coastal Flooding Caused by Extreme Coastal Water Level at the World Heritage Historic Keta City (Ghana, West Africa). *J. Mar. Sci. Eng.* **2023**, *11*, 1144. [CrossRef]
40. Orton, P.; Lin, N.; Gornitz, V.; Colle, B.; Booth, J.; Feng, K.; Buchanan, M.; Oppenheimer, M.; Patrick, L. New York City Panel on Climate Change 2019 Report Chapter 4: Coastal Flooding. *Ann. N. Y. Acad. Sci.* **2019**, *1439*, 95–114. [CrossRef] [PubMed]
41. USACE. *Eastwick Stream Modeling and Technical Evaluation-Levee Flood Protection*; U.S. Army Corps of Engineers: Philadelphia, PA, USA, 2014.
42. AKRF. *Lower Eastwick Infrastructure and Flood Evaluation: Hydrology and Hydraulic Modeling—Existing Conditions Flood Model*; AKRF: Philadelphia, PA, USA, 2021.
43. Princeton Hydro. *Lower Darby Creek Hydrologic and Hydraulic Analysis Report*; Princeton Hydro: Philadelphia, PA, USA, 2017; Volume 5660.
44. Beffa, C.; Connell, R.J. Two-Dimensional Flood Plain Flow. I: Model Description. *J. Hydrol. Eng.* **2001**, *6*, 397–405. [CrossRef]
45. Akanbi, A.A.; Katopodes, N.D. Model for Flood Propagation on Initially Dry Land. *J. Hydraul. Eng.* **1988**, *114*, 689–706. [CrossRef]
46. Mita, K.S.; Orton, P. Eastwick Compound Flood Model: V2. Available online: https://data.mendeley.com/datasets/3wjvmymf68/2 (accessed on 18 April 2023).
47. Lian, J.J.; Xu, K.; Ma, C. Joint impact of rainfall and tidal level on flood risk in a coastal city with a complex river network: A case study of Fuzhou City, China. *Hydrol. Earth Syst. Sci.* **2013**, *17*, 679–689. [CrossRef]
48. Torres, J.M.; Bass, B.; Irza, N.; Fang, Z.; Proft, J.; Dawson, C.; Kiani, M.; Bedient, P. Characterizing the hydraulic interactions of hurricane storm surge and rainfall–runoff for the Houston–Galveston region. *Coast. Eng.* **2015**, *106*, 7–19. [CrossRef]
49. PASDA Open GIS Data Access for the Commonwealth of Pennsylvania. Available online: https://www.pasda.psu.edu (accessed on 12 June 2023).
50. NCEI Coastal Digital Elevation Model-1/9 Arc-Second Resolution Bathymetric-Topographic Tiles. Available online: https://maps.ngdc.noaa.gov/viewers/bathymetry/?layers=dem (accessed on 10 April 2023).
51. NOAA Nautical Chart. Chart 12311: Delaware River, Smyrna River to Wilmington; Chart 12312: Delaware River, Wilmington to Philadelphia; Chart 12313: Delaware River, Philadelphia and Camden Waterfronts. Available online: www.charts.noaa.gov/ChartCatalog/MidAtlantic.html (accessed on 10 April 2023).
52. USGS Water Data for the Nation. Available online: https://waterdata.usgs.gov (accessed on 4 July 2023).
53. NOAA Tides and Currents. Available online: https://tidesandcurrents.noaa.gov (accessed on 4 July 2023).
54. Multi-Resolution Land Characteristics (MRLC) Consortium. Available online: https://www.mrlc.gov/ (accessed on 4 July 2023).
55. USACE HEC-RAS River Analysis System User's Manual Version 6.0. Available online: https://www.hec.usace.army.mil/confluence/rasdocs/rasum/6.1 (accessed on 7 April 2023).
56. Arcement, G.J.; Verne, R.S. *Guide for Selecting Manning's Roughness Coefficients for Natural Channels and Flood Plains*; Water Supply Paper 2339; U.S. Geological Survey: Reston, VA, USA, 1989. Available online: https://pubs.usgs.gov/wsp/2339 (accessed on 20 July 2023).

57. Stedinger, J.R.; Vogel, R.M.; Foufoula-Georgiou, E. Frequency Analysis of Extreme Events. In *Handbook of Hydrology*; Maidment, D., Ed.; McGraw-Hill Book Co.: New York, NY, USA, 1993; pp. 18.1–18.66.
58. Suro, T.P.; Deetz, A.; Hearn, P. *Documentation and Hydrologic Analysis of Hurricane Sandy in New Jersey, October 29–30, 2012*; Scientific Investigations Report 2016-5085; U.S. Geological Survey: Reston, VA, USA, 2016. [CrossRef]
59. USACE. *Darby and Cobbs Watersheds Hydrologic Study*; U.S. Army Corps of Engineers: Philadelphia, PA, USA, 2016.
60. Blumberg, A.F.; Georgas, N.; Yin, L.; Herrington, T.O.; Orton, P.M. Street-Scale Modeling of Storm Surge Inundation along the New Jersey Hudson River Waterfront. *J. Atmos. Ocean. Technol.* **2015**, *32*, 1486–1497. [CrossRef]
61. Strauss, B.H.; Orton, P.M.; Bittermann, K.; Buchanan, M.K.; Gilford, D.M.; Kopp, R.E.; Kulp, S.; Massey, C.; de Moel, H.; Vinogradov, S. Economic damages from Hurricane Sandy attributable to sea level rise caused by anthropogenic climate change. *Nat. Commun.* **2021**, *12*, 2720. [CrossRef]
62. Wang, W.; Zhou, K.; Jing, H.; Zuo, J.; Li, P.; Li, Z. Effects of Bridge Piers on Flood Hazards: A Case Study on the Jialing River in China. *Water* **2019**, *11*, 1181. [CrossRef]
63. Costabile, P.; Macchione, F.; Natale, L.; Petaccia, G. Flood mapping using LIDAR DEM. Limitations of the 1-D modeling highlighted by the 2-D approach. *Nat. Hazards* **2015**, *77*, 181–204. [CrossRef]
64. Pareja-Roman, L.F.; Chant, R.J.; Sommerfield, C.K. Impact of Historical Channel Deepening on Tidal Hydraulics in the Delaware Estuary. *J. Geophys. Res. Oceans* **2020**, *125*, e2020JC016256. [CrossRef]
65. Lee, S.B.; Li, M.; Zhang, F. Impact of sea level rise on tidal range in Chesapeake and Delaware Bays. *J. Geophys. Res. Oceans* **2017**, *122*, 3917–3938. [CrossRef]
66. Pareja-Roman, L.F.; Orton, P.M.; Talke, S.A. Effect of Estuary Urbanization on Tidal Dynamics and High Tide Flooding in a Coastal Lagoon. *J. Geophys. Res. Oceans* **2023**, *128*, e2022JC018777. [CrossRef]
67. AKRF. *Lower Eastwick Infrastructure and Flood Evaluation: Hydrology and Hydraulic Modeling—Boundary Condition & Event Analysis*; AKRF: Philadelphia, PA, USA, 2021.
68. Ashley, R.; Blanksby, J.; Chapman, J. Towards Integrated Approaches to Reduce Flood Risk in Urban Areas. In *Advances in Urban Flood Management*; CRC Press: Boca Raton, FL, USA, 2007; pp. 427–444, ISBN 9780429224348.
69. Bogodi, J. The Search for the Lost Flood Culture: The International Flood Initiative. In *Floods, from Defence to Management*; Van Alphen, J., Van Breek, E., Taal, M., Eds.; Taylor & Francis Group: London, UK, 2005; pp. 507–512, ISBN 0415380502.
70. Hay, J.; Mimura, N. Supporting climate change vulnerability and adaptation assessments in the Asia-Pacific region: An example of sustainability science. *Sustain. Sci.* **2006**, *1*, 23–35. [CrossRef]
71. Conway, D.; Schipper, E.L.F. Adaptation to climate change in Africa: Challenges and opportunities identified from Ethiopia. *Glob. Environ. Chang.* **2011**, *21*, 227–237. [CrossRef]